Density Functional Study of Ethylene Hydrogenation on Pt(111) Surface

Toshiko Miura,[†] Hisayoshi Kobayashi,*[,†] and Kazunari Domen[‡]

Department of Chemical Technology, Kurashiki University of Science and the Arts, 2640 Tsurajima, Nishinoura, Kurashiki, 712-8505 Japan, and Research Laboratory of Resources Utilization, Tokyo Institute of Technology, 259 Nagatsuda, Midori-ku, Yokohama 227, Japan

Received: September 24, 1999; In Final Form: March 8, 2000

The mechanism of ethylene hydrogenation on Pt surfaces has been investigated using the density functional method and the Pt_n cluster models ($n = 7$, 10) modeling the Pt(111) surface. The energetics were investigated along the overall hydrogenation reactions: adsorption of ethylene onto the hydrogen preadsorbed Pt cluster, successive H atom migrations to adsorbed ethylene, and formation of ethane. Among the configurations considered here, the di-σ and π configurations gave the local minima. The di-σ configuration was found to be more stable than the π configuration for both the hydrogen free and preadsorbed surfaces. The calculated activation energy was larger for the second hydrogenation. Both the di-σ and π configurations lead to a common product, surface ethyl, from which the second hydrogenation occurs. The surface ethyl produced ethane in the eclipsed conformation, which was desorbed from the surface. Although the hydrogenation from the di-σ configuration is energetically favorable for clean surfaces, the energetics considerably depends on the coadsorbed surface species such as hydrogen atom and carbon deposit, and on the real catalysts, both reactions will proceed comparably.

Introduction

There is a long history of research for the hydrogenation of unsaturated hydrocarbon molecules on the noble metals. In 1970s, development of the electron spectroscopies and their application to the surface phenomena established a new research field called "surface science". Characterization of small molecules, especially unsaturated hydrocarbon species adsorbed on the transition metal surfaces is one of the most exciting subjects.[1,2] There are many papers reporting the adsorption of ethylene and acetylene on Pt and Pd surfaces. The structures of adsorbed species were discussed in terms of the di-σ and π configurations for the beginning, and then replaced with the ethylidyne ($\equiv C-CH_3$) or ethylidene ($=CH-CH_3$) species, which were easily formed on surfaces.[3,4] However, the latter species have recently been found to be too stable to be active intermediates for catalytic reactions, such as hydrogenation, and reexamination has started with new experimental techniques.[5−9]

On the other hand, several papers of theoretical calculations have been published. Earlier works on ethylene/Pt systems reported were the extended Hückel type calculations.[10−12] In these studies, the chemisorption interactions were interpreted in terms of the orbital interactions between the adsorbate and surface,[10,11a] and the surface arrangement of adsorbate was discussed with the periodic boundary conditions.[11b,12] There are more elaborate calculation for similar systems. Fahmi and van Santen examined stable structures of acetylene and ethylene on Ni(111).[13] Clotet and Pacchioni reported adsorption sites and vibrational frequencies of acetylene on Cu and Pd(111).[14] Very recently, density functional (DF) studies have been reported for ethylene/Pt systems. Shen et al. reported ethylene adsorption onto SiO_2 supported Pt and PtSn surfaces.[15] Ge and King investigated adsorption and dissociation to ethylidyne on Pt-(111) using the plane wave DF method.[16] In the present article, we discuss relative stability among the sites and the hydrogenation mechanisms on Pt(111) surface on the basis of the accurate total energy calculation.

Method of Calculation and Models

The gradient corrected DF method was employed in this calculation. The functionals used were the Slater[17] and Becke exchange[18] and Lee−Yang−Parr correlation functionals[19] (BLYP). The Gaussian 98 program was used throughout the work.[20] Los Alamos model core potentials (MCP)[21] and corresponding basis sets were used for Pt atoms as implemented in this program.[20] Two MCP sets are implemented in Gaussian 98 program: one is large core (1s to 5p) and small valence (5d6s6p) set, and the other is small core (1s to 4p) and large valence (5s5p5d6s6p) set. The use of latter is recommended. However, we dealt with relatively large clusters and the transition state (TS) structures for which the SCF convergence was rather difficult due to many low lying virtual orbitals at the elongated bond lengths. We employed the large core-small valence set for all the calculations with the Pt_7 cluster and the geometry optimization with the Pt_{10} cluster. For the Pt_{10} cluster, the total energy is reevaluated with the small core-large valence set after the optimization. For H and C atoms, Dunning−Huzinaga full double-ζ (D95) basis sets were used.[22]

We employed hexagonal shaped Pt_7 and Pt_{10} clusters modeling the Pt(111) surface. The Pt_{10} cluster includes three second layer Pt atoms as well as seven first layer atoms in Pt_7 cluster. In the preliminary calculations using the Pt_7 model, relative stability for adsorbed ethylene is compared among the six configurations: di-σ, two types of π, μ-bridge, and two types of triangular ones. Throughout this work, the Pt clusters are fixed, and the structure and relative orientation of ethylene molecule and hydrogen atoms with respect to the Pt cluster is optimized. The stabilization energy is defined as $\Delta E = \{E(\text{Pt cluster}) + E(C_2H_4) + xE(H_2)\} - E(\text{combined system})$, where

[†] Department of Chemical Technology.
[‡] Research Laboratory of Resources Utilization.

10.1021/jp993425k CCC: $19.00
Published on Web 06/30/2000

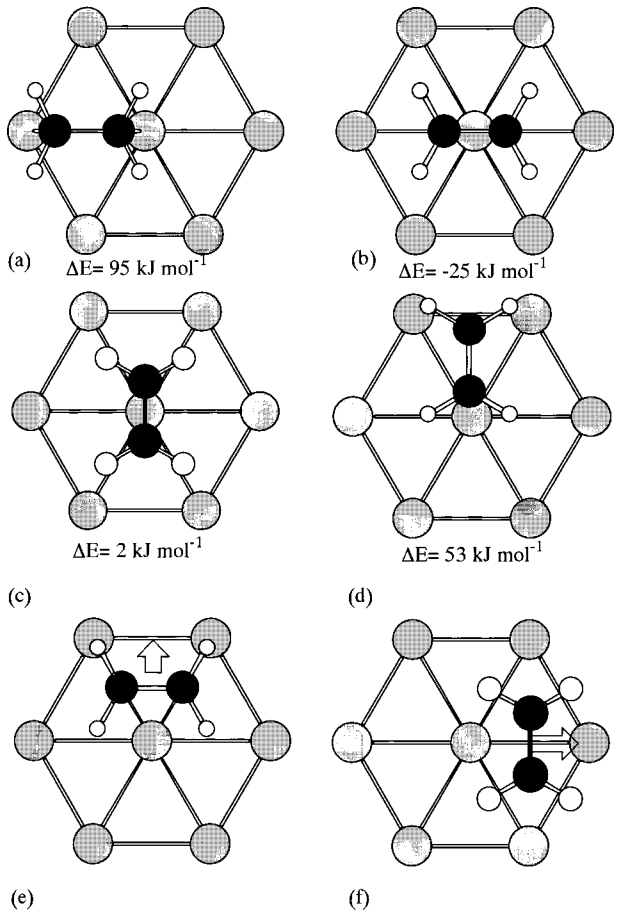

Figure 1. Six configurations of ethylene on Pt_7 cluster. Large core-small valence basis set is used.

$x = {}^1/_2$ or 1 depending on the number of H atoms in the system. ΔE is shown as positive values for stable adsorption. All the calculations were carried out at the lowest spin multiplicity, i.e., singlet or doublet, which were found to have the lowest total energies.

Results and Discussion

Preliminary Calculation with Pt_7 Cluster. Six configurations of adsorption ethylene examined for the preliminary calculation are shown in Figure 1. The di-σ configuration (Figure 1a) gives the largest stabilization energy of 95 kJ mol^{-1}. Two π configurations are shown in Figure 1b and c, and are designated as parallel and perpendicular configurations, respectively. With the Pt_7 cluster, the parallel configuration is unstable, and ethylene slightly binds for the perpendicular configuration. Figure 1 shows the (d) perpendicular and (e) parallel triangular configurations. The former gives an optimized structure with a stabilization energy of 53 kJ mol^{-1}, but the latter continuously changes to the di-σ configuration with the two peripheral Pt atoms. The μ-bridge configuration (shown in Figure 1f) has not a local minimum and again changes to the π configuration with the peripheral Pt atom. The stabilization energy decreases in the order of di-σ, triangular, and π configurations.

Ge and King presented adsorption energies of 107, 60, and 53 kJ mol^{-1} for the di-σ, triangular, and π configurations, respectively.[16] (Their naming of sites is translated to ours.) These values are compared with 95, 53, and 2 kJ mol^{-1}, respectively, and the relative order is consistent with each other. Shen et al. refer the values of 116 and 71 kJ mol^{-1} for adsorption to the Pt_{19} cluster,[15] and Fahmi and van Santen also suggest the di-σ configuration for the ethylene/Ni(111) system.[13] Thus, the di-σ configuration is definitely more stable species though the π configuration is less stabilized compared to other works.

The structure of perpendicular triangular configuration (shown in Figure 1d) is obtained from the di-σ one by rotation of 30 degree around the central Pt atom, and their reaction mechanisms will resemble each other. In the following, we investigate the hydrogenation mechanism with the two typically different configurations, i.e., the di-σ and π configurations.

Adsorption to Clean Pt(111) Surface Modeled by Pt_7 and Pt_{10} Clusters. The optimized structures of ethylene for the di-σ and two π configurations using Pt_{10} cluster are shown in Figure 2. The adsorption energies are compared between the Pt_7 (see Figure 1) and Pt_{10} clusters. With the Pt_{10} cluster, the adsorption energy decreases to about half for the di-σ configuration, whereas it increases to values of 21−25 kJ mol^{-1} for the π configurations. Larger cluster seems to decrease the difference between the sites. Although the absolute energies are dependent on cluster size considerably, the di-σ configuration is more stable than the π configurations. Between the two π configurations, the parallel orientation is more stable slightly, and we investigate the hydrogenation mechanism with the parallel one.

The π configurations are optimized only with the symmetry constraint. Small deviation from its symmetrical orientation leads to the di-σ or triangular configurations. In other words, two di-σ sites or two triangular sites symmetrically exist in both sides of the π site, and the π configuration itself is thought to be the TS for translation from one di-σ (or triangular) configuration to the other. Its energy barrier is estimated to be 31 kJ mol^{-1}. From the energetics, it is safe to say that the di-σ configuration is first fulfilled for adsorption at the clean surfaces.

First Hydrogenation through di-σ Configuration: Pt_x-H + $C_2H_4 \rightarrow Pt_x + C_2H_5$. The optimized structures of reactant, TS, product and shifted product, and their energies are shown in Figures 3 and 6. At the reactant shown in Figure 3a, ethylene is adsorbed to the central and peripheral Pt atoms, and the H atom to the Pt atom at the opposite end. The minimum energy pass is traced adopting the C−H distance as the approximate reaction coordinate. From the structure with the highest energy on the minimum energy pass, the TS is searched allowing all coordinates to change. We confirmed at the obtained TS structure (Figure 3b) that the number of negative eigenvalues of Hessian matrix is one. The calculated TS energy is below the zero energy level by 16 kJ mol^{-1}, and the barrier height measured from the reactant is 81 kJ mol^{-1}.

Through TS, the reaction leads the product where the C atom is bonded to the peripheral Pt atom with a stabilization energy of 150 kJ mol^{-1} (Figure 3c). To check site dependency between the central and peripheral Pt atoms, the C_2H_5 moiety in the product is shifted so that the C atom is bonded to the central Pt atom, and the structure is re-optimized, as shown in Figure 3d. The energy differences between the product and "shifted product" are 40 kJ mol^{-1}, and the peripheral Pt atom is more "active" to the bonding. This energy is not small and the use of larger clusters is clearly desirable. However, the activation energy is free from this inhomogeneity since the structural change between the reactant and TS is small. Furthermore, we recognize that the reaction is only slightly exothermic comparing the reactant with the shifted product. In Figure 6, the energy profiles are shown for both the Pt_7 /small valence basis set and Pt_{10}/large valence basis set. The first difference is a large reduction of the TS barrier by 72 kJ mol^{-1} for the latter calculation model. On the other hand, the inhomogeneity of clusters becomes explicit for the latter.

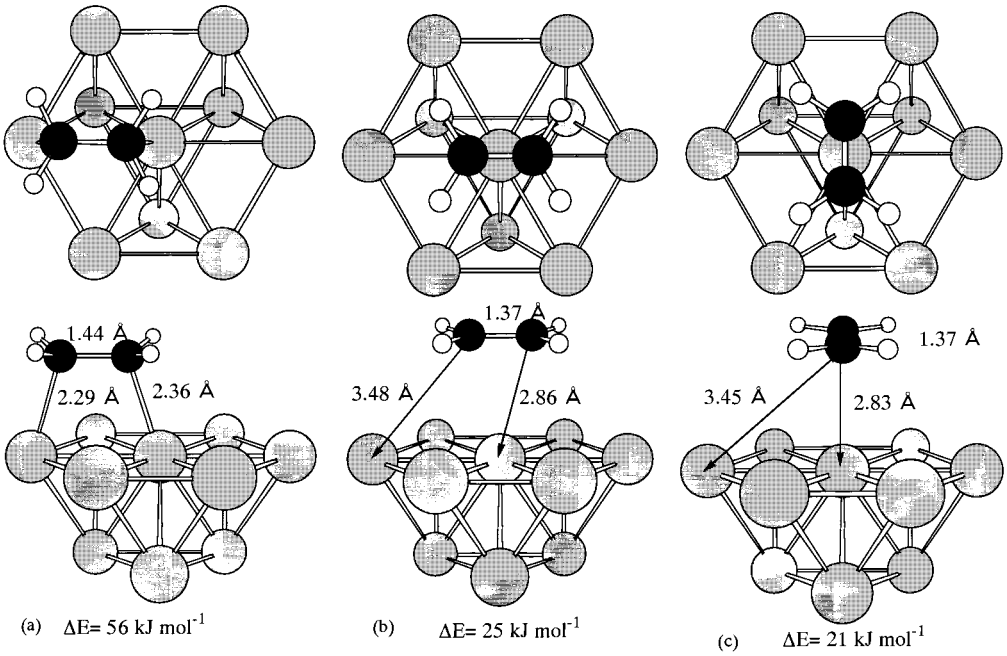

Figure 2. Optimized structures of ethylene on Pt_{10} cluster. Energy is re evaluated with small core-large valence basis set after the structures are optimized. (a) di-σ configuration, (b) parallel π configuration, and (c) perpendicular π configuration.

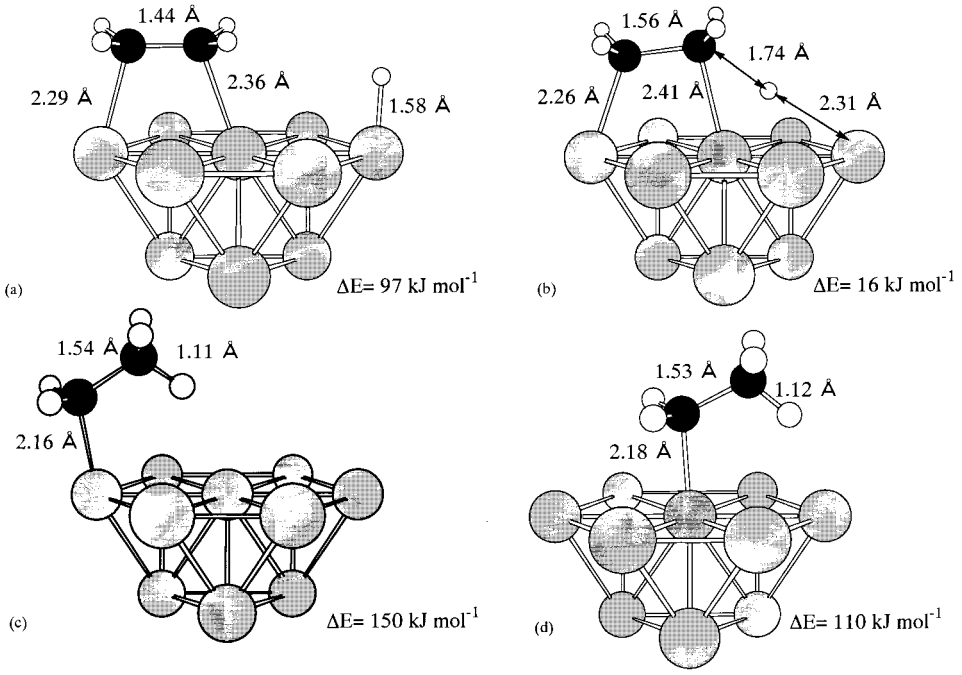

Figure 3. Structures and energy profile for $Pt_{10}-H + C_2H_4 \rightarrow Pt_{10} + C_2H_5$ reaction with di-σ configuration. (a) Reactant, (b) transition state, (c) product, and (d) shifted product.

Available data for the heat of adsorption is very limited. Velic and Levis reported 92 kJ mol^{-1} for the π configurations on the Pt(111) with atomic oxygen.[7] We expect that oxygen covered Pt surfaces are more active than the pure Pt surface, since the $Pt + C_2H_4 + H_2$ system is electron excessive and the electron withdrawing by oxygen is convenient for strong bonding. Their value is close to our value estimated for the di-σ configuration. Shen Zaera estimated 117 kJ mol^{-1} for the sum of adsorption energy of C_2H_4 and H_2.[6] Shen et al. reported 125 kJ mol^{-1} for adsorption on Pt/SiO_2 by their microcalorimetric measurement.[15] These values are consistent with our calculated adsorption energies.

First Hydrogenation through π Configuration: Pt_x-2H + $C_2H_4 \rightarrow Pt_x$-H + C_2H_5. In the reactant, the ethylene is adsorbed to the $Pt_{10}H_2$ cluster, where two H atoms are bonded to the two peripheral Pt atoms. The reactant is optimized under the C_s symmetry, as shown in Figure 4a. The local minimum is obtained but its energy is above the zero level by 8 kJ mol^{-1}. This means that the ethylene-Pt interactions on the H covered surface are very weak in the π configuration. This negative adsorption energy is not ascribed to the activated adsorption of ethylene but to the instability of H_2/Pt_{10} system. In our separate calculations, we found that the second H atom is not adsorbed stably and decreases the total adsorption energy.[23] The indirect

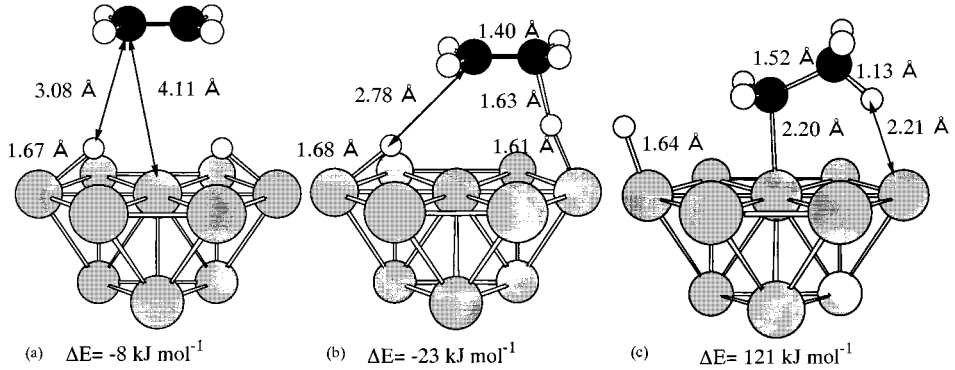

Figure 4. Structures and energy profile for Pt_{10}-2H + C_2H_4 → Pt_{10}−H + C_2H_5 reaction with π configuration. (a) Reactant, (b) transition state, (c) product.

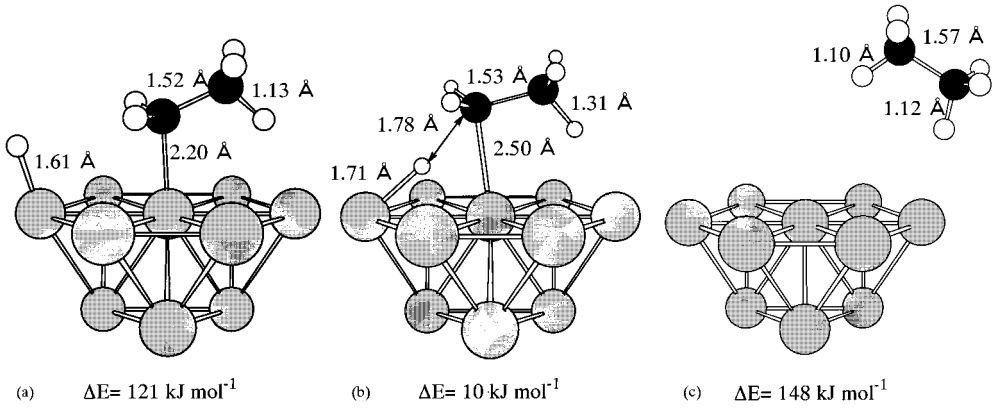

Figure 5. Structures and energy profile for Pt_{10}−H + C_2H_5 → Pt_{10} + C_2H_6 reaction. (a) Reactant, (b) transition state, (c) product.

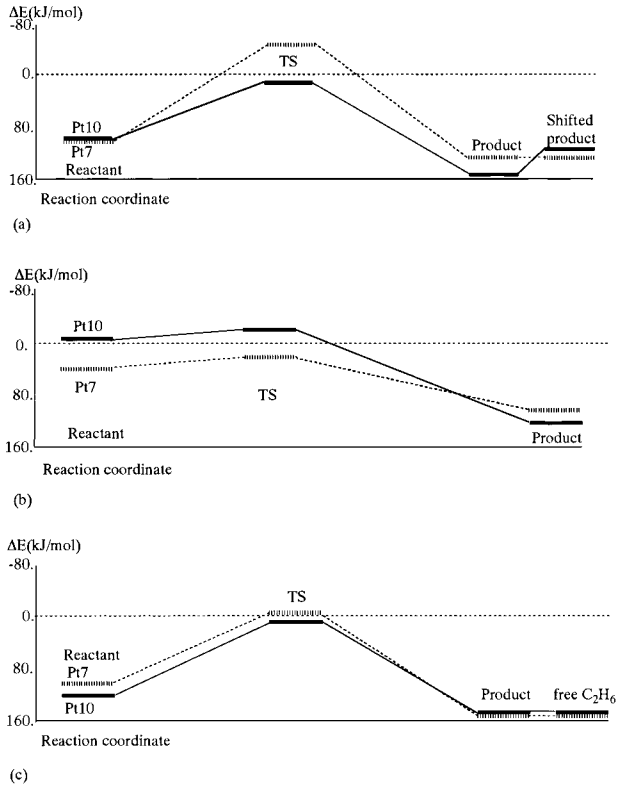

Figure 6. Energy profiles along the three reactions. Solid lines show results with Pt_{10} cluster and small core-large valence set, and dotted lines show preliminary results with Pt_7 cluster and large core-small valence set. (a) First hydrogenation through di-σ ethylene, (b) first hydrogenation through π ethylene, and (c) second hydrogenation through surface ethyl group.

adsorbate−adsorbate repulsive interactions are expected between two H atoms on Pt surfaces. Ethylene moiety is slightly shifted to the either direction to break the symmetry. The reaction proceeds as if ethylene falls down on the H−Pt bond, and the H atom is taken in ethylene. The TS is searched in the same way as the di-σ configuration, and the structure is shown in Figure 4b. The calculated TS energy is 23 kJ mol^{-1} above the zero level, and the activation barrier measured from the reactant is only 15 kJ mol^{-1}. The product is the surface ethyl bonded to the central Pt atom and the H atom bonded to the peripheral Pt atom as shown in Figure 4c. It is interesting that the H atom is bent back to the opposite side to the surface ethyl. Figure 6b shows difference in the calculation models. The activation barrier calculated with the Pt_7 cluster is 20 kJ mol^{-1} and the relative energies are shifted upward almost uniformly for the reactant and TS. On the other hand, the product is more stabilized with the Pt_{10} cluster. Since the energy of surface ethyl and H (product of Figure 6b) should be lower than the energy of surface ethyl only (shifted product of Figure 6a), the result of the Pt_{10} cluster is more reasonable.

Second Hydrogenation through Surface Ethyl: Pt_x-H + C_2H_5 → Pt_x + C_2H_6. The optimized structure for the reactant is shown in Figure 5a, and this structure is the product itself (as shown in Figure 4c) for the first hydrogenation through π configuration, and is also very similar to the shifted product (as shown in Figure 3d) for the first hydrogenation through di-σ configuration except for the second added H atom. Comparing the energies between the shifted product (ΔE = 110 kJ mol^{-1}) and the reactant (ΔE = 121 kJ mol^{-1}), the stabilization energy for H atom bonded to the (active) peripheral Pt atom is estimated to be 11 kJ mol^{-1}. In our reaction model, both the di-σ and π configurations lead to a common product, the surface ethyl

group, and so the reaction mechanism for second hydrogenation is common and unique.

The structure of TS is shown in Figure 5b, and its energy is calculated to be 10 kJ mol^{-1} below zero level and the barrier height measured from the reactant is 111 kJ mol^{-1}. This barrier is the highest among the three reactions considered. The reason is ascribed to large stability of the surface ethyl group. After the TS, ethane is produced in an eclipsed conformation, and desorbed from the cluster (as shown in Figure 5c). The cited energy is not for the optimized adsorption system but the sum of free ethane and free surface. The energy profile is shown in Figure 6c, and differences between the two calculation models are very small. The reactant, TS, and product are, respectively, more stabilized by 18, 15, and -3 kJ mol^{-1}.

General Discussion and Comparison with Experimental Results. We have investigated the energy profile and structural changes along the hydrogenation of ethylene on Pt surface. The di-σ configuration is energetically preferable and fulfilled selectively on the surface when the two adjacent sites are available. The di-σ configuration results in larger adsorption energy and higher activation barrier than the π configuration. On the contrary, the π configuration could be existed as an intermediate even though the surface coverage is high and a single site is available for ethylene. Ethylene in the π configuration is bound very weakly to the Pt cluster. However, the activation barrier is also very low, and adsorbed ethylene and H atom produce the surface ethyl in almost down hill reaction. These calculation results agree well with the recent experimental results by Somorjai's group.[5] They observed both configurations of ethylene on Pt(111), but they think the π configuration is a main intermediate for hydrogenation.

Finally, we stress that the first hydrogenation starting from the di-σ or π configuration leads to the same product, surface ethyl group, and therefore the second hydrogenation proceed through a common mechanism discussed above. Comparison of the activation barrier between the first (di-σ and π) and second hydrogenation steps was a question in long controversy. Our calculation estimates 81, 15, and 111 kJ mol^{-1} of the activation barriers measured from the corresponding reactants, and indicates that the second hydrogenation is the rate-determining step. Zeara reported values of 63 and 25 kJ mol^{-1} for activation energies of the first and second hydrogenation,[6] and Domen et al. reported a value of 37 kJ mol^{-1} as an apparent activation energy.[9b] Compared to Zeara's estimate, the stability of surface ethyl group seems to be overestimated, which results in the larger activation energy for the second hydrogenation. However, we think that the surface ethyl is reasonably stable since a tight C−H bond is formed at the cost of more weak H−Pt and C−Pt bonds. Calculated activation energies are much larger than the experimental estimates. One reason is smallness of the clusters used. However, a whole discrepancy is not responsible for the calculation. The activation energies calculated from the potential energy surface correspond to "cold" reactant, where the energy gained by prior hydrogenation or adsorption is completely dispersed. Under real reaction conditions, whole reaction proceed as rapid as the energy dissipation. The excess heat of formation for the surface ethyl is retained within the molecular moiety as the vibrational energy (for which we call "hot" reactant). This energy could be used as a part of the activation energy for the second hydrogenation, which leads to reduction of the apparent activation energy. This energy preservation mechanism works only partly, otherwise apparent activation energy becomes 0 and 23 kJ mol^{-1} for the di-σ and π configurations.

Somorjai's group thought the π configuration is a real intermediate,[5] whereas Domen et al. did not detect the π configuration in their recent works.[9] We still think that, in realistic surfaces of metal catalysts, the π configuration has more advantage as the active intermediate since the number of available surface sites, especially adjacent multiatom sites is more limited due to the carbon deposit and decomposed fragments as well as preadsorbed hydrogen atoms. The calculated result that the reactant is bound very weakly is rather consistent with the Domen's recent experimental finding.[9] It is not excluded that this reaction occurs very quickly through the π configuration, and the π configuration is not detected by the spectroscopic methods.

Thus, we think that our calculation offered a better understanding of the reaction profile, i.e., structures of intermediates and energy changes along the reactions although the absolute values of energies calculated in the present work even depend on the basis sets and cluster models adopted.

The hydrogenation mechanism on real surfaces and catalysts was much more complicated than expected. Since the total energies are also sensitive to the other coadsorbed species, such as adsorbed hydrogen atoms, ethylidyne, and carbon deposits, those influences should be considered together in future works.

Acknowledgment. This work is a part of the project of the Institute for Fundamental Chemistry, supported by the Japan Society of the Promotion of Science Research for the Future Program (JSPS-RFTF96P00206). This research was supported by the Grant-in Aid for Scientific Research on Priority Areas "Molecular Physical Chemistry(403)" from the Ministry of Education, Science, Sports, and Culture.

References and Notes

(1) For reviews, see: (a) Bertolini, J. C.; Massardier, J. In The Chemical Physics of Solid Surfaces and Heterogeneous Catalysis; King, D. A., Woodruff, D. P., Eds.; Elsevier: New York, 1984; Vol. 3, Part B. (b) Brown, W. A.; Kose, R.; King, D. A. *Chem. Rev.* **1998**, *98*, 797.

(2) Ibach, H.; Hopster, H.; Sexton, B. *Appl. Surf. Sci*. **1977**, *1*, 1.

(3) Kesmodel, L. L.; Dubois, L. H.; Somorjai, G. A. *Chem. Phys. Lett*. **1978**, *56*, 267.

(4) Demuth, J. E. *Surf. Sci*. **1979**, *80*, 367.

(5) (a) Cremer, P. S.; Somorjai, G. A. *J. Chem. Soc., Faraday Trans*. **1995**, *19*, 3671. (b) Cremer, P. S.; Su, X.; Shen, Y. R.; Somorjai, G. A. *J. Am. Chem. Soc*. **1996**, *118*, 2942.

(6) Zaera, F. *Langmuir* **1996**, *12*, 88.

(7) Velic, D.; Levis, R. J. *J. Chem. Phys*. **1996**, *104*, 9629.

(8) Döll, R.; Gerken, C. A.; Van Hove, M. A.; Somorjai, G. A. *Surf. Sci*. **1997**, *374*, 151.

(9) (a) Ohtani, T.; Kubota, J.; Kondo, J. N.; Hirose, C.; Domen, K. *Surf. Sci. Lett*. **1998**, *415*, L983. (b) Ohtani, T.; Kubota, J.; Kondo, J. N.; Hirose, C.; Domen, K. *J. Phys. Chem. B* **1999**, *103*, 4562.

(10) Anderson, A. B.; Hubbard, A. T. *Surf. Sci*. **1980**, *99*, 384.

(11) (a) Gavezzotti, A.; Simonetta, M. *Surf. Sci*. **1980**, *99*, 453. (b) Ditlevsen, P. D.; Van Hove, M. A.; Somorjai, G. A. *Surf. Sci*. **1993**, *292*, 267.

(12) Maurice, V.; Minot, C. *Langmuir* **1989**, *5*, 734. (b) Maurice, V.; Minot, C. *J. Phys. Chem*. **1990**, *94*, 8579.

(13) Fahmi, A.; van Santen R. A.*Surf. Sci*. **1997**, *371*, 53.

(14) Clotet, A.; Pacchioni, G. *Surf. Sci*. **1996**, *346*, 91.

(15) Shen, J.; Hill, J. M.; Watwe, R. M.; Spiewak, B. E.; Dumesic J. A. *J. Phys. Chem*. **1999**, *103*, 3923.

(16) Ge, Q.; King, D. A. *J. Chem. Phys*. **1999**, *110*, 4699.

(17) Slater, J. C. *Phys. Rev*. **1951**, *81*, 385.

(18) Becke, A. D. *Phys. Rev*. **1988**, *A38*, 3098.

(19) Lee, C.; Yang, W.; Parr, R. G. *Phys. Rev*. **1988**, *B37*, 785.

(20) Frisch, M. J.; Trucks, G. W.; Schlegel, H. B.; Scuseria, G. E.; Robb, M. A.; Cheeseman, J. R.; Zakrzewski, V. G.; Montgomery, J. A., Jr.; Stratmann, R. E.; Burant, J. C.; Dapprich, S.; Millam, J. M.; Daniels, A. D.; Kudin, K. N.; Strain, M. C.; Farkas, O.; Tomasi, J.; Barone, V.; Cossi, M.; Cammi, R.; Mennucci, B.; Pomelli, C.; Adamo, C.; Clifford, S.; Ochterski, J.; Petersson, G. A.; Ayala, P. Y.; Cui, Q.; Morokuma, K.; Malick, D. K.; Rabuck, A. D.; Raghavachari, K.; Foresman, J. B.; Cioslowski, J.;

Ortiz, J. V.; Stefanov, B. B.; Liu, G.; Liashenko, A.; Piskorz, P.; Komaromi, I.; Gomperts, R.; Martin, R. L.; Fox, D. J.; Keith, T.; Al-Laham, M. A.; Peng, C. Y.; Nanayakkara, A.; Gonzalez, C.; Challacombe, M.; Gill, P. M. W.; Johnson, B.; Chen, W.; Wong, M. W.; Andres, J. L.; Gonzalez, C.; Head-Gordon, M.; Replogle, E. S.; Pople, J. A. *Gaussian 98*, Revision A.5; Gaussian, Inc.: Pittsburgh, PA, 1998.

(21) (a) Hay, P. J.; Wadt, W. R. *J. Chem. Phys*. **1985**, *82*, 270. (b) Wadt, W. R.; Hay, P. J. *J. Chem. Phys*. **1985**, *82*, 284. (c) Hay, P. J.; Wadt, W. R. *J. Chem. Phys*. **1985**, *82*, 299.

(22) Dunning, T. H., Jr.; Hay, P. J. In *Modern Theoretical Chemistry*; Schaefer, H. F., III, Ed.; Plenum Press, New York, 1976; p 1.

(23) Miura, T.; Kobayashi, H.; Domen, K. In preparation.